JALS Vol.1 n.1
Journal of Applied and Laser Spectroscopy 2014

Analysis of Multispectral Images in Cultural Heritage and Archaeology

E. Salerno [1], A. Tonazzini [1], E. Grifoni [2], G. Lorenzetti [2], S.Legnaioli [2], M. Lezzerini [3], L. Marras [4], S. Pagnotta [2], V. Palleschi [2,5]

[1]Institute of Science and Technologies of Information, Research Area of CNR, Via G. Moruzzi, 1 – 56124 PISA
[2]Laboratory of Applied and Laser Spectroscopy, Institute of Chemistry of Organometallic Compounds, Research Area of CNR, Via G. Moruzzi, 1 – 56124 PISA
[3]Department of Earth Sciences, University of Pisa, Via S. Maria 53 - 56126 PISA (Italy)
[4]Art-Test di Luciano Marras e C. s.a.s., Via del Martello 14, 56121 PISA (Italy)
[5]Department of Civilizations and Forms of Knowledge, University of Pisa, Via L. Galvani 1 - 56126 PISA (Italy)

Received 28 July 2014, accepted 10 August 2014

Abstract

This paper presents a discussion on different techniques that can be used for the analysis of multispectral images (i.e., images taken in more than three spectral bands) that are acquired in the context of Cultural Heritage or Archaeological studies. False Color imaging, Blind Source Separation methods and techniques based on the use of Artificial Neural Networks are discussed. Examples are presented on the application of these methods to the study of Cultural Heritage and Archaeology.

1. Introduction

Multispectral imaging is one of the most diffused techniques for the study of Cultural Heritage and Archaeological paintings[1-5]. Although the spectral resolution of this kind of analysis is, in general, very limited, the amount of information that can be obtained is extremely high, considering the high spatial resolution of the images that can be obtained with very simple experimental setups.

In its simpler application, multispectral imaging implies the acquisition of color and, typically, infrared images in at least four spectral bands (three in the visible region, RGB, and one in the infrared, Ir). Although most of the statistical methods that will be discussed in this paper could be, in principle, applied to less, more, or different spectral bands, even the minimum set of RGB and Ir images is a good example of how multispectral imaging can provide an information not visible to the eye (infrared band) that is not trivial to visualize together with the RGB visible information.

Several technique have been proposed, in the last decades, for extracting from a set of multispectral images information on the materials used for the realization of the painting[6-9] or for evidencing hidden patterns through the elaboration of the digital images[10-11].

The approaches normally used imply the reduction of the number of bands to be visualized to three, for exploiting the possibility of visualizing the result as a (false) color image[13-16] or in any case a linear combination of the multispectral images for evidencing patterns and similarities[10-11,17]. Most of these methods can be applied using blind algorithms, which operates automatically without the intervention of an operator[18-23].

In the following, we will discuss the applications of the main statistical methods used, with a specific attention to the study of Cultural Heritage and Archaeological paintings.

2. Techniques for the Analysis of Multispectral sets of images

2.1 False color imaging

The problem of visualizing in color a set of images acquired in more than three spectral bands (typically Blue (B: 400-450 nm), Green (G: 450-550 nm), Red (R: 550-650 nm) and Infrared (Ir > 700 nm)) is usually solved in the simplest way, i.e. getting rid of one of the three images acquired in the visible and using the other two plus the infrared for building a (false) color image. The

Corresponding author: Vincenzo Palleschi, e-mail: vincenzo.palleschi@cnr.it
Keywords: Cultural Heritage, Archeology, Multispectral analysis.

canonical way of doing this substitution practically corresponds to a shift of the spectral bands towards the Infrared. The Blue image is discarded and substituted with the image in the Green band, the Green image is substitute with the Red and the Red is substituted with the Infrared (IrRG false color imaging). An example of this procedure is shown in figure 1, using a set of images acquired on a detail of the painting of Ghirlandaio "The Crowning of the Virgin", conserved at the Palazzo Eroli Museum in Narni (TR).

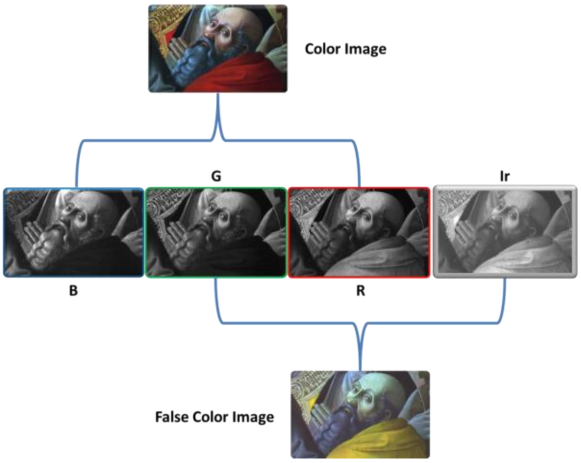

Figure 1: Color (RGB) and False Color Images (IrRG).

It's worth noting that, although there is a general agreement, among the operators in the field, in identifying the False Color Image with the IrRG subset of the multispectral images, in fact many other 'False Color' images can be built, according to the specific needs. The most used 'non-canonical' False Color images that can be built from a set of four are the IrGB False Color (the Red image is replaced with the Infrared, this approach has the advantage of giving a more realistic restitution of the colors) and the Infrared inverse False Color Image, which is a canonical False Color image in which the Infrared band is substituted by its negative ($\overline{Ir}$RG). This last False Color image is particularly suited for enhancing underdrawings and *pentimenti* in paintings, since the black lines in the Infrared are transformed in bright red lines, using this kind of restitution. The only practical advantage of using the canonical False Color approach (IrRG) instead of other False Color restitutions is the availability of reference materials that have been already studied, in the past, with this kind of imaging[6-7,9]. It is commonly believed that some kind of identification of the pigments can be obtained from the False Color associated to them. In most cases, this color is given, essentially, by the red component of the False Color image (Infrared band); however, this component is extremely sensitive to the structure of the painted layer, due to the characteristic of Infrared radiation of penetrating under the surface (if the pigment is at least partially transparent at this wavelength). Therefore, the qualitative identification of pigments through their color in the False Color image is in general problematic, and should be discouraged in common practice when there is the evidence of a superposition of different painted layers that could interact in a complex way with the infrared radiation.

2.2 *Chromatic derivative imaging*

The Chromatic Derivative Imaging (ChromaDI) is a variant of False Color imaging which is obtained through the subtraction of consecutive couples of spectral images, as schematically shown in figure 2 (detail of a roman painted sarcophagus, III century A.D.)

The method was introduced by the authors[24] with the intent of building a False Color image which would take into account the information from all the multispectral images acquired, without excluding *a priori* one of the four images in the multispectral set (the method can also be generalized to multispectral sets with more than 4 images). The ChromaD Image gives information on the changes in reflectivity of the object with the wavelength; with respect to the canonical False Color Imaging, the differences between the optical behavior of the various pigments is exalted, taking into account the changes occurring while passing from the shorter wavelengths (blue band, which is more sensitive to the surface details) to the longer ones (green and red bands) in the visible image.

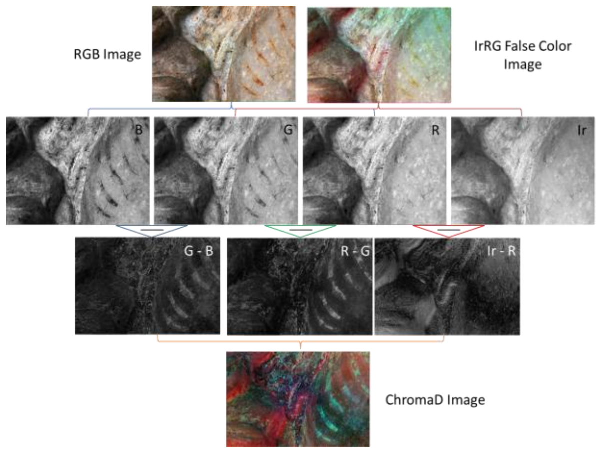

Figure 2: ChromaD Image construction.

1.1 2.3 *Blind separation methods*

Blind separation methods are typically applied for the unsupervised separation of features in the multispectral image set that are not immediately apparent in the corresponding Color/False Color/ChromaD images. A simple assumption is that the observed images result from the superposition of individual patterns that combine linearly to form the final appearance. If ***x(i,j)*** is an N-vector map representing the multispectral image and ***s(i,j)*** is an M-vector map representing the collection of the original patterns, we can assume that

$$\boldsymbol{x}(i,j) = \boldsymbol{A}\boldsymbol{s}(i,j) \qquad (1)$$

where *(i,j)* is the pixel index and the N×M-matrix ***A*** is called mixing matrix. Blind separation techniques consist in estimating ***s*** from the multispectral data ***x***, making assumptions of statistical nature. For example, the elements of vector ***s*** can be considered as mutually independent, non-Gaussian random variables. This leads to the class of separation techniques denoted as Independent Component Analysis (ICA)[20-21]. Alternatively, uncorrelatedness rather than independence can be imposed [23-24]. This leads to the Principal Component Analysis techniques[27] (PCA), through which a set of N multispectral channels produces N images representing mutually uncorrelated patterns.

The sets of images ***s(i,j)*** produced by ICA or PCA are often much more readable than the original multispectral images. Each output image carries information from the entire multispectral set, and is likely to highlight patterns with peculiar spectral signatures that are not represented in the others.

An example application of PCA analysis to a mural painting of an Etruscan tomb in Chiusi (Siena) is shown in figure 3. A multispectral set of six images, taken in the RGB bands plus three Infrared bands (centered around 850, 950 and 1050 nm, respectively) was used as input. Note that there is no association between the PCA images and the bands where the original multispectral images were acquired, since each output of the Blind Separation Technique is a linear combination of all the input images. However, it seems also clear that each output image brings a different information from the others.

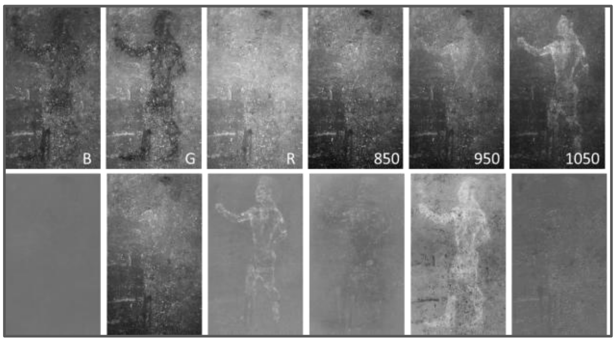

Figure 3: PCA separation of the upper set of multispectral images.

The third image from the left, in the output, is particularly interesting because it shows the evidence of a small vase in the right hand of the figure, which is very difficult to distinguish even in the Infrared image taken at 1050 nm, the most readable of the multispectral images. The comparison of the two images is shown in figure 4.

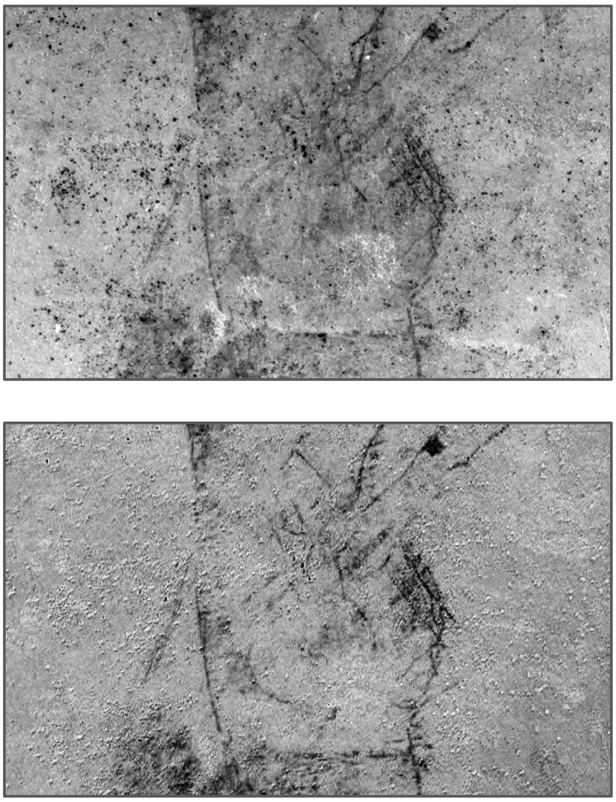

Figure 4: Up: Infrared (1050 nm) image; Down: One of the PCA outputs from the multispectral channel set. The images are shown in negative for exalting the contours.
Similar results can be obtained imposing different statistical constraints on the images *s* (Orthogonalization, ICA[24]).

A possible alternative approach implies a different definition of the concept of 'similarity' between the spectral signatures in the multispectral images set. A way of representing the multispectral image set is as a two-dimensional spatial structure, defined by the pixel index (i,j), where each pixel is associated to an N-dimensional vector whose components are the pixel intensities in the corresponding spectral images. In other words, as in conventional color imaging each pixel is associated with a three dimensional vector whose components are its intensities in the Red, Green and Blue bands, in multispectral imaging an N-vector is associated to each pixel, with components corresponding to the intensity of the same pixel in the N channels.

The distance *d* between two N-dimensional vectors x and x', associated to different pixels (i,j) and (i',j'), can be defined as either the Euclidean distance:

$$d = \sqrt{\sum_{k=1}^{N} (x_k - x_k')^2} \qquad (2)$$

or the spectral angle between them, commonly used in remote sensing applications[30]:

$$d = \cos^{-1}\left(\frac{x \cdot x'}{|x||x'|}\right) \qquad (3)$$

The difference between these two definitions is crucial and has to be carefully considered, as the first definition sees as 'distant' vectors representing similar (hyper)colors with different intensities, while the second discriminates the vectors according to the similarity of their associated (hyper)colors, independently on their intensities.

An example where the definition (3) can be more useful than (2) involves the manual selection of a pixel in the image and the automatic identification of all the other pixels that have 'similar' colors, after a proper proximity threshold is set. This approach requires the supervision of the operator, but has the advantage of being more selective with respect to a fully automatic separation technique. The application of this technique to the previous painting is shown in figure 5. The pixels marked in yellow are the ones showing an optical behavior similar to that of the figure's hair, within a threshold angle between the hypercolor vectors of 30 degrees.

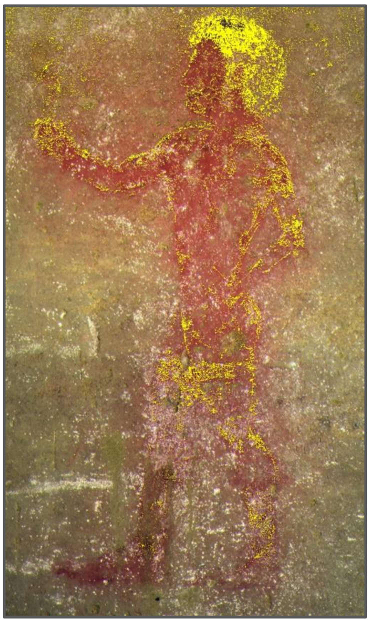

Figure 5: Identification of the pixels showing an optical behavior similar to that of the figure's hair (angle between the hypercolor vectors < 30 degrees).

From the observation of figure 5 it can be seen that the outline of the figure was probably realized with the same pigment used for the hair of the figure. This is not immediately evident in the original multispectral images, nor in the images obtained using the PCA method.

2.4 Neural Networks Analysis

The analysis of multispectral images can be performed using another unsupervised method based on Artificial Neural Networks[26], called Kohonen Self-Organizing Map (SOM)[27]. The SOM Network is a self-organized Neural Network that consists of neurons representing a N-dimensional weight vector, where N is the dimension of the multispectral (hyper)vector. The pixels in the image are assigned to the node which is 'closer' to their (hyper)color. The different neurons adjust their weights (hypercolors) in order to get the largest possible number of pixels, in a competitive way. The SOM method is particularly suited for classification purposes[28-29], since each neuron of the map is associated to samples that are in some way different from the ones associated to the other neurons. From a practical point of view, the number of neurons in the map is chosen in order to cover the chromatic variations in the image to be analyzed. An example of the application of this method is given on the anonymous XVI century painting shown in figure 6, representing a scene of the Plague in Sansepolcro.

Figure 6: The Plague in Sansepolcro, oil on wood (Anonymous, XVI century).

The output of a 3x3 SOM, obtained from a set of four images (RGB+Infrared) of the painting, is shown in figure 7.

The SOM approach can be used for identifying in the painting the zones corresponding to pigments which shows a similar optical behavior. The technique is fast and works in a fully automatic way. Since the SOM method implies the calculation of distances between (hyper)colors, different results might be obtained according to the definition of distance used (eq. (2) or eq. (3)). Note that, contrarily to the Blind Separation Methods discussed in the previous subsection, the number of SOM nodes can be larger than the number of input images. Each pixel in the image is associated to one and only one neuron, whose associated weights can be interpreted as the components of the hypercolor vector associated to the centroid of their distribution; the number of pixels associated to each neuron can be small or large, depending on the neuron color, and a 'distance' between the neurons can be defined, which indicates how different are, in fact, their colors in the SOM.

Figure 7: *The Plague in Sansepolcro*, oil on wood (Anonymous, XVI century). The distance between colors is defined according to eq. (2).

The images corresponding to each node are in Black and White, since the single pixels can be associated to the corresponding neuron (White) or not (Black). These images can be colorized in different hues (arbitrarily), and merged together in a single (false color) segmented image, as shown in figure 8, where each color marks the pixels with similar optical behavior.

CONCLUSIONS

Multispectral imaging sets can be analyzed in many different ways, starting from the direct observation of the single images or through a simple reduction method as False Color Imaging. More sophisticated methods, such as ChromaD Imaging and Blind Separation Methods, imply the application of linear transformations on the original multispectral images. These latter Blind Methods depend on the definition of a distance among (hyper)colors, that can be chosen to be Euclidean or being related to the angle between the (hyper)vectors representing the optical behavior of the materials under study. Finally, non-linear methods based on the use of Artificial Neural Networks can be applied to obtain a segmentation of the image according to the different pigments used.

None of the methods presented here is *a priori* better than the others. According to the specific situation under study, one or more methods can be more informative than others. Due to the intrinsic simplicity of the numerical treatment, different approaches can be easily tested and compared, to obtain a better readability of the images and, consequently, a better understanding of the optical properties of the object under study, exploiting at the best the power of the multispectral imaging techniques.

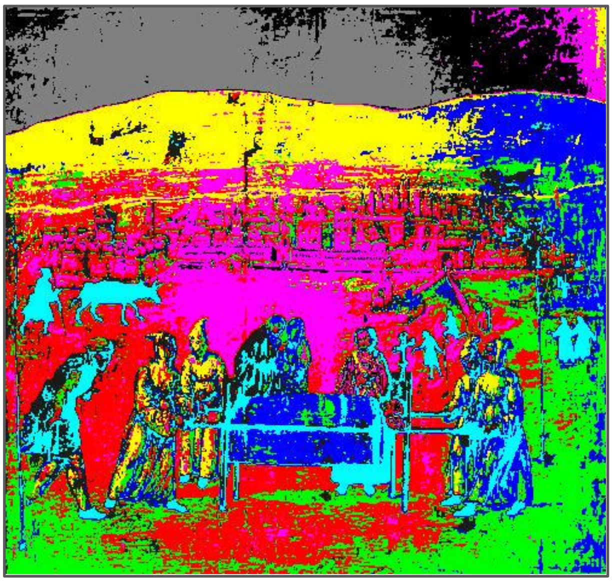

Figure 8: Segmentation in false colors of the painting in figure 6, according to the SOM results shown in figure 7.

ACKNOWLEDGEMENTS

ES and AT are partially supported by European funds, through the program POR Calabria FESR 2007-2013 - PIA Regione Calabria Pacchetti Integrati di Agevolazione Industria Artigianato Servizi, project ITACA (Innovative Tools for cultural heritage ArChiving and restorAtion).

REFERENCES AND NOTES

[1] Marengo, E., Manfredi, M., Zerbinati, O., Robotti, E., Mazzucco, E., Gosetti, F., Bearman, G., France, F., Shor, P., Development of a technique based on multi-spectral imaging for monitoring the conservation of cultural heritage objects, *Analytica Chimica Acta*, **2011**, *706*, 2, 229-237.

[2] Bonifazzi, C., Carcagnì, P., Fontana, R., Greco, M., Mastroianni, M., Materazzi, M., Pampaloni, E., Pezzati, L., Bencini, D., A scanning device for VIS-NIR multispectral imaging of paintings, *Journal of Optics A*, **2008**, *10*, 6, art. no. 064011.

[3] Paviotti, A., Forsyth, D.A., Cortelazzo, G.M., Lightness recovery for pictorial surfaces, *International Journal of Computer Vision*, **2011**, *94*, 1, 54-77.

[4] Li, S.-Y., Manabe, Y., Chihara, K., Color and gloss reproduction from multispectral images, *Proceedings of SPIE*, **5667**, art. no. 21, pp. 170-177.

[5] Toque, J.A., Ide-Ektessabi, A., Investigation of the degradation mechanism and discoloration of traditional

Japanese pigments by multispectral imaging, *Proceedings of SPIE*, **2005**, *7869*, art. no. 78690E.

[6] Toque, J.A., Sakatoku, Y., Ide-Ektessabi, A., Pigment identification by analytical imaging using multispectral images, *Proceedings of the International Conference on Image Processing,* **2009**, art. no. 5414508, 2861-2864.

[7] Melis, M., Miccoli, M., Quarta, D., Multispectral Hypercolorimetry and automatic guided pigment identification: Some masterpieces case studies, *Proceedings of SPIE*, **2013**, *8790*, art. no. 87900W.

[8] Comelli, D., Nevin, A., Valentini, G., Osticioli, I., Castellucci, E.M., Toniolo, L., Gulotta, D., Cubeddu, R., Insights into Masolino's wall paintings in Castiglione Olona: Advanced reflectance and fluorescence imaging analysis, *Journal of Cultural Heritage*, **2011**, *12*, 1, 11-18.

[9] Ricciardi, P., Delaney, J.K., Glinsman, L., Thoury, M., Facini, M., De La Rie, E.R., Use of visible and infrared reflectance and luminescence imaging spectroscopy to study illuminated manuscripts: Pigment identification and visualization of underdrawings, *Proceedings of SPIE*, **2009**, *7391*, art. no. 739106.

[10] Legnaioli, S., Grifoni, E., Lorenzetti, G., Marras, L., Pardini, L., Palleschi, V., Salerno, E., Tonazzini, A., Enhancement of hidden patterns in paintings using statistical analysis, *Journal of Cultural Heritage*, **2013**, *14*, (3 SUPPL), S66-S70.

[11] Easton Jr., R.L., Christens-Barry, W.A., Knox, K.T., Spectral image processing and analysis of the Archimedes Palimpsest, *European Signal Processing Conference*, **2011**, 1440-1444.

[12] Mazzeo, R., Palazzi, C.E., Roccetti, M., Sciutto, G., Computer-assisted pigment identification in artworks, *Proceedings of the IASTED European Conference on Internet and Multimedia Systems and Applications*, **2007**, 266-271.

[13] Rogerio-Candelera, M.A., Jurado, V., Laiz, L., Saiz-Jimenez, C., Laboratory and in situ assays of digital image analysis based protocols for biodeteriorated rock and mural paintings recording, *Journal of Archaeological Science*, **2011**, *38*, 10, 2571-2578.

[14] Daffara, C., Pampaloni, E., Pezzati, L., Barucci, M., Fontana, R., Scanning multispectral IR reflectography SMIRR: An advanced tool for art diagnostics, *Accounts of Chemical Research*, **2010**, *43*, 6, 847-856.

[15] Fontana, R., Gambino, M.C., Greco, M., Marras, L., Materazzi, M., Pampaloni, E., Pezzati, L., Poggi, P., New high resolution IR-colour reflectography scanner for painting diagnosis, *Proceedings of SPIE*, **2003**, *5146*, 108-115.

[16] Delaney, J.K., Zeibel, J.G., Thoury, M., Littleton, R., Morales, K.M., Palmer, M., De La Rie, E.R., Visible and infrared reflectance imaging spectroscopy of paintings: Pigment mapping and improved infrared reflectography, *Proceedings of SPIE*, **2009**, *7391*, art. no. 739103.

[17] Hollmann, J.C., Crause, K., Digital imaging and the revelation of 'hidden' rock art: Vaalekop Shelter, KwaZulu-Natal *Southern African Humanities*, **2011**, *23*, 1, 55-76.

[18] Feng, S., Shijie, C., Mohammad-Djafari, A., Bayesian blind separation of mixed text patterns, *Proceedings of the 2008 International Conference on Audio, Language and Image Processing*, **2008**, art. no. 4590212, 1373-1378.

[19] Tonazzini, A., Gerace, I., Martinelli, F., Multichannel blind separation and deconvolution of images for document analysis, *IEEE Transactions on Image Processing*, **2010**, *19*, 4, art. no. 5356171, 912-925.

[20] Tonazzini, A., Bedini, L., Salerno, E., Independent component analysis for document restoration, *International Journal on Document Analysis and Recognition*, **2004**, **7**, 17–27.

[21] Hyvärinen, A., Karhunen, J., Oja, E., *Independent component analysis*, John Wiley, New York (2001).

[22] Bell, A.J., Sejnowski, T.J., An information-maximization approach to blind separation and blind deconvolution, *Neural Computation*, **1995**, *7*, 1129–1159.

[23] Cichocki, A., Amari, S.I., *Adaptive blind signal and image processing*, Wiley, New York (2002)

[24] Legnaioli, S., Lorenzetti, G., Cavalcanti, G.H., Grifoni, E., Marras, L., Tonazzini, A., Salerno, E., Pallecchi, P., Giachi, G., Palleschi, V., Recovery of archaeological wall paintings using novel multispectral imaging approaches, *Heritage Science*, **2013**, *1*, 1, art. no. 33.

[25] Wold, S., Esbensen, K., Geladi, P., Principal component analysis, *Chemometrics and Intelligent Laboratory Systems*, **1987**, *2*, 1-3, 37-52.

[26] Haykin, S.S., Neural networks. A comprehensive foundation, Second Edition, Prentice-Hall, New Jersey, U.S (1999).

[27] Kohonen, T., The self-organizing map, *Proceedings of the IEEE*, **1990**, *78*, 9, 1464-1480.

[28] Kuncheva, L.I., *Combining pattern classifiers: Methods and algorithms*, Wiley Interscience, New Jersey, U.S. (2004).

[29] Villmann, T., Merényi, E., Hammer, B., Neural maps in remote sensing image analysis, *Neural Networks*, **2003**, *16,* 3-4, 389-403.

[30] Dennison, P.E., Halligan, K.Q., Roberts, D.A., A comparison of error metrics and constraints for multiple endmember spectral mixture analysis and spectral angle mapper, *Remote Sensing of Environment*, **2004**, *93*, 3, 359-367.